

## Experimental and numerical study of pressure ratio distributions for transonic condensing flow through a stationary stator blades cascade

**Dr. Reyadh Ch. Al-Zuhairy**

Ministry of Higher Education and Scientific Research/ Baghdad.

Email:reyadhc@yahoo.com

**Dr. Muwafag Sh. Alwan**

Electromechanical Engineering Department ,University of Technology/Baghdad.

**Abd-Alamer D. Zidan**

Institute of Technology/ Baghdad.

Received on:31/8 /2014 & Accepted on:29/1/2015

### Abstract

In the course of expansion in turbines steam nucleates to become a two phase mixture, the liquid consisting of a very large number of extremely small droplets carried by the vapor. Formation and subsequent behavior of the liquid lowers the performance of turbine wet stages. The calculations were carried out assuming that the flow is two dimensional, compressible, turbulent and viscous. A classical homogenous nucleation model applied for the mass transfer in the transonic conditions. The aim of the present study is investigation of outlet pressure effect on second phase generation in a steam turbine. The conditions at inlet to the test section were varied from a wet equilibrium to a superheated state by changing the cascade exit pressure. Experimentally it was found that the most important influence of rapid condensation on the pressure distribution is occurred on the suction surface and it grows by decreasing the downstream pressure. Pressure profiles around the blades are compared with the experimental data and good agreement is observed. The maximum and minimum of droplet numbers have been achieved and nucleation zone has been specified in blade passage.

### دراسة عملية وعددية لتوزيع نسبة الضغط لجريان تكثيفي حول صوتي لصف من الريش الثابتة

#### الخلاصة

خلال مرحلة التمدد التي تحدث في المراحل الأخيرة للتوربينات البخارية ذات الضغط الواطي يبدأ البخار بالتكثيف ليصبح خليط ذو طورين، الطور السائل يتكون من عدد هائل من القطرات الصغيرة جدا والتي تكون منقولة بواسطة الطور الغازي. عملية تكوين القطرات وسلوكها تؤدي إلى تقليل الأداء والكفاءة للمراحل الأخيرة لهذا النوع من التوربينات مما يؤدي إلى انخفاض الكفاءة بصورة عامة. جميع الحسابات تمت بفرض ان الجريان ثنائي الأبعاد، انضغاطي، مضطرب، ولزج. وباستخدام نظرية التثوي المتجانس لانتقال الكتلة في الجريان حول الصوتي. الهدف من الدراسة الحالية هو معرفة تأثير ضغط الخروج على تولد الطور الثاني (الطور السائل) في

<https://doi.org/10.30684/etj.33.5A.11>

2412-0758/University of Technology-Iraq, Baghdad, Iraq

This is an open access article under the CC BY 4.0 license <http://creativecommons.org/licenses/by/4.0>

التوربينات البخارية. شروط الجريان الداخل لمقطع الفحص ممكن تغييرها من الرطوبة المتزنة إلى درجة التخميص بواسطة تغيير ضغط الخروج.  
عمليا وجد أن التأثير الرئيسي للتكثيف الفجائي يحدث في سطح السحب للريشة ويزداد وينمو كلما يقل ضغط الخروج. تمت مقارنة توزيع الضغوط على سطوح الريشة عمليا ونظريا والنتائج أظهرت تقارب كبير بينهما، كما تم إيجاد وحساب أكبر وأقل عدد للقطرات وتحديد مكان حدوثه خلال مجرى الجريان.

### Nomenclature

c	Blade chord, m.
$c_x$	Blade axial chord, m.
I	Nucleation rate, No. nuclei/m <sup>3</sup> .s.
k	Turbulent kinetic energy, m <sup>2</sup> /s <sup>2</sup> .
M	Mach number
P	Pressure, bars.
S	Super saturation ratio.
r	Radius of the droplet, m.
R	Gas constant, N/kg.K
V	Droplet volume, m <sup>3</sup> .
x	Axial coordinate, m.
$x/c_x$	Fraction of surface distance.
$\beta$	The wetness mass fraction.
$\Gamma$	Mass generation rate due to condensation and evaporation, Kg/m <sup>3</sup> .s.
	Number of liquid droplets per unit volume.
$\eta$	Dissipation of turbulent kinetic energy, m <sup>2</sup> /s <sup>2</sup> .
$\varepsilon$	Density, or mixture density, kg/m <sup>3</sup> .
$\rho$	Liquid surface tension, N/m.
$\sigma$	

### Subscript and Superscript

b	back
g	Gaseous –phase consisting of water vapor
l	Liquid –phase consisting of condensed water droplets
o	Stagnation conditions.
*	critical
-	Average.

### INTRODUCTION

In the large steam turbines used for electrical power production, the steam enters the low-pressure (Lp) turbine cylinders as a dry superheated vapor but exhausts to the condenser as a two-phase mixture of saturated vapor and small liquid droplets. Within the blade passages, the liquid droplets are formed mainly by homogeneous nucleation as the vapor becomes highly supersaturated due to the rapid expansion process. Once formed, the droplets grow rapidly, but the rate of expansion in the blade passages is generally so high that thermodynamic equilibrium is only established in the inter-row gaps and in the final turbine exhaust diffuser leading to the condenser.

Departures from equilibrium are manifest by differences in temperature between the droplets and the vapor and by the fact that the wetness fraction of the two-phase mixture differs from the equilibrium value corresponding to the local pressure and entropy. Velocity slip between the phases also occurs but, for the submicron sized

droplets which constitute the main bulk of the liquid phase, this is much less significant than the effects of thermal non-equilibrium. There are two main reasons why departures from thermal equilibrium in steam turbines are important. **First**, the heat and mass transfer between the vapor and liquid phases can have a strong effect on the flow behavior within the blade passages. This is particularly marked in the final (Lp) turbine stages where the flow becomes supersonic and generates shock waves which can interact in a most complex way with the processes of droplet nucleation and growth. **Second**, non-equilibrium condensation is a thermodynamically irreversible process resulting in the production of entropy which, ultimately, translates into a reduction in turbine efficiency. The loss in turbine efficiency due to wetness has never been precisely quantified.

Progress in experimentation has been less satisfactory. Wet-steam is a difficult medium in which to obtain measurements and most of the data used for validation purposes have been obtained in simple one-dimensional nozzle experiments [1]. Initially, the only measurements technically possible were of the axial static pressure distribution through the (misleadingly named) 'condensation shock', but these provided insufficient data to fix empirically the unknown parameters in the theoretical models. Subsequently, a great advance in instrumentation was made by the introduction of an optical technique for measuring the wetness properties [2]. This has now been developed to such an extent that wetness fraction and mean droplet size data can be obtained, not only in laboratory nozzles, but also in operational machines [3]. In many cases, the actual number distribution of droplet sizes can also be inferred by numerically inverting the optical transmission data [4]. The current situation is that agreement between theory and experiment for steady and periodically oscillating flows in one-dimensional nozzles is generally satisfactory. Almost no experimental data is available, however, for the case of two-dimensional condensing flow in stationary cascades of turbine blades and this is the area addressed by the present paper.

Many experimental investigations into the performance of the wet stages of turbines do not offer completely quite enough satisfactory means of investigating the influence of the individual factors that contribute to wetness losses. Also because of most of the previous testing has been performed in air due to extra difficulties associated with contamination of instrumentation and flow visualization by condensation and long thermal settling time between condition changes. To reproduce turbine nucleating and wet flow conditions requires a supply of supercooled steam; this can be achieved easily under blow-down facility by the equipment employed according to [5]. The existing results obtained by [5 & 6] confirm that nucleating flows exhibit features that are absent from superheated flows.

### **Experimental Investigation**

The experimental work was developed to provide means for validating the theoretical predictions of wet steam nucleation and to understand the mechanisms that cause the extra losses due to nucleation. A comprehensive description of the experimental facilities given by [Ref. \[6\]](#) and [Ref \[7\]](#) were found to be very helpful for the present work to design experimental test rig which can be used to investigate wet steam nucleation in a last stage of steam turbine cascade blade.

Experimental study was prepared for non-equilibrium condensing transonic steam flow in a stationary cascade of last stage stator turbine blade. The conditions at inlet to the test section could be varied from a wet equilibrium to a superheated state by adjusting the cascade exit pressure. One of the problems rise in this research is how to

obtain steam of properties for last stage of steam turbine which is of vacuum pressure down to 0.5 bar and temperature range change (75-100 C). For the above reason an expansion drum has been used instead of the turbine to overcome the high expansion rate of the steam, and to obtain the required amount, pressure, temperature and condition of the steam (i.e. steam at zone close to saturation vacuum pressure).

The drum also has many functions such that: it is working as absorb of the steam flow disturbance and the pressure fluctuating that exiting from the orifices tube of the expansion drum. This process leads to obtain uniform flow in test section. The drum size was selected suitable large enough to satisfy the above requirements. The drum has a cylindrical shape with two ended cups as shown in figure (1) parts (6) and (7). The drum diameter is 0.9 m and the drum height is 2m with addition of the two cups gave 1.271 m<sup>3</sup> sizes. The steam entering the expansion drum from the upper end through a 1.6 m length vertical perforated pipe mounted inside the drum with diameter of 76.2 mm, the perforated pipe contain of 47 orifices with diameter of 6 mm. These orifices working as a chocking device to the steam flow.

The size and number of orifices were calculated assuming isentropic steam flow and chocking condition exist at the orifice outlet and by using the isentropic, chocked flow rate relation where the Mach number equal unity. The chocked condition is true where as the critical pressure at the orifice outlet is greater than drum pressure.

According to the principle of the isentropic and chocked flow (M = 1) through the orifices, the number and sizes of holes can be calculated using the following relation [7]:

$$\left(\frac{\dot{m}}{A}\right)_{max.} = \frac{\dot{m}}{A_{Orifice}^*} = \frac{P_o}{\sqrt{T_o}} \sqrt{\frac{\gamma}{R}} \left(\frac{2}{\gamma+1}\right)^{\frac{\gamma+1}{\gamma-1}} \quad \dots (1)$$

Where

,  $\dot{m}$  is the steam flow rate (kg/sec),  $T_o$  is the steam stagnation temperature,  $P_o$  is the steam stagnation pressure,  $A^*$  orifice is the orifice area (hole diameter),  $\gamma = 1.32$  and  $R$  are the steam constants. With respect to the steam conditions entering the expansion drum after passing throttling valve the total orifices area was found to be 0.0010967 m<sup>2</sup>.

By choosing a suitable orifice diameter of 6 mm, the number of orifices was found equal to 39, the condensation ratio in the drum was found experimentally to be approximately of about 20%. The measured amount in a certain time of condensation steam in the drum is subtracted from the total amount of the steam flow rate in the system. Therefore mass flow rate of steam entering the test section is of about 160 kg/h. The number of required orifices can be obtained by choosing a suitable orifice diameter of 6 mm and by using the following relation:

$$A_{Orifice}^* = \frac{\pi}{4} (d^2) \times N \quad \dots (2)$$

So that, the required number of orifices was found to be approximately 47 holes.

### Experimental Facilities

The schematic diagram of the general arrangement and main components of the expansion drum facility are shown in Fig. (1). Steam was supplied to the test section from boiler via, throttling valve, flow regulation valve, and expansions drum. Steam is supplied at 10 bars, 186 °C, and maximum steam flow rate is 200 kg/h. The steam conditions at inlet to the test section can be varied from a wet equilibrium to a superheated state by adjusting the water pass through the boiler and amount of steam entering and leaving the expansion drum. The flow leaving the test section is passing to

a condenser. By varying the cooling water flow rate in the condenser and vacuum pump, the test section pressure ratio and hence the exit Mach number can be controlled. The mass flow rate available from the boiler limited the number and size of blades to four, thus providing only three passages. This is the minimum number that could be used for an acceptable validation of computer code incorporating periodic boundary condition modeling a finite cascade [6]. The blade profile selected for the experiments is a geometrically a copy of a fifth stage stator blade from the last stage of low pressure steam turbine. This profile is chosen because experiments previously conducted in the actual turbine had indicated high losses in the fifth stage which corresponded to the location of the primary nucleation. Also a comparison between the present and existing results of [5,6] can be done easily since both results were done for identical cascade blade.

The three blade passages were formed from two aluminum blades and two half profile aluminum blades. The upper and lower halves represent the pressure and suction surfaces of the blade respectively. The two sides of the test section was constructed from 10 mm thickness pure glass (98% purity) to permit a clear vision of the physical changes in the fluid properties especially at the trailing edge region. Fig.(2) Shows the cascade test section arrangement.

To obtain uniform flow at cascade intake, steam was entered the test section via a converging nozzle and two parallel sides with exit dimensions identical to the cascade inlet cross sectional area. The depth of the test section was selected as 26 mm, giving a blade aspect ratio of (1.1). The test section was staggered by an angle of (45.32°) to simulate the real steam turbine blade staggered angles. The exit design Mach number is (M = 1.2) and the outlet flow angle about 71°. All the characteristic values of cascade can be evaluated as listed in Table (1). To carry out the surface pressure measurements, tapping were drilled into the blade surfaces (pressure and suction); also the wall tapping were drilled along the middle passage line starting from upstream to downstream of the cascade. The measuring points of the static pressure at the middle of the cascade passage are design to give pressure distribution along the mid span of the passage. This pressure distribution gives a clear picture of the Mach number distribution along the middle passage. Pressure lines were lead out from the test section via steel tubing contained within cascade frame and measurements were made using a multi tube differential manometer connected to the tapping's by a series arrangement.

**Table (1) characteristic values of cascade**

Blade axial chord	23.07 mm
Blade pitch	21.8 mm
Blade chord	32.8 mm
Stagger angle	45.32°
Inlet flow angle	0.0°
Outlet flow angle	71.0°
Solidity	1.5
Span or blade height	26 mm
Aspect ratio	1.1
Throat	7.1 mm

### **Numerical Investigation**

A number of numerical studies were directed toward modeling two phase flow behavior of nucleating steam. Much of this modeling work was initially conducted on two dimensional flows in turbine cascade; in this regard the numerical approaches most

often used have been the single phase, inviscid, and time-marching scheme of Denton for turbo-machinery flows as done by [8-13]. Using these approaches gives limitations on extending these methods to more complex flow conditions involving nucleation steam. With more sophisticated numerical models used that contains the viscous and turbulence effects as made by [12-15]. Therefore additional information about two phase flow behavior of nucleating steam can be achieved. A model for homogeneous nucleation in high-speed transonic flow applicable to the wet stages of a steam turbine has been presented by many researchers such as [11]. At the present work attention is restricted to the behavior of homogeneous nucleation. The equations governing droplet nucleation and growth can be combined with the field conservation equations and the behavior of nucleating and two-phase flows analyzed. The Eulerian-Eulerian approach was adopted for modeling the condensing steam flow. And the two-phase flow is modeled using the conservation-type two-dimensional compressible Navier-Stokes equations, with the transport equations for the liquid-phase mass-fraction and the number of liquid droplets per unit volume. Under the foregoing assumptions, the mixture flow is governed by the compressible Navier-Stokes equations. The mixture pressure, temperature and velocity components are obtained by solving Navier-Stokes equations using a second-order spatially accurate density-based flow algorithm. This algorithm employs a coupled algebraic multigrid to accelerate a two-sweep point implicit Gauss-Seidel relaxation scheme. CFD code Fluent 12.1 is implemented within a full Navier-Stokes viscous flow solution procedure, employs a density based finite volume discretization of the governing equations of fluid motion.

In the two dimensional case a correct definition of boundary conditions is even more difficult than in the one dimensional case. In addition to the inlet and the outlet boundary conditions, the solid wall and the periodic boundary are necessary for calculating the flow through a turbine blade cascade, Fig. (3) Shows the boundary conditions.

The passage geometry considered in the present work is a fifth stage low pressure steam turbine stator blade; it is identical to passage generated in the experimental test rig.

To perform simulations of the system on a computer, the partial differential equations (i.e. the transport equations) need to be discretized, resulting in a finite numbers of points in space at which variables such as velocity, pressure are calculated. The usual methods of discretization, such as finite volumes, use neighboring points to calculate derivatives, and so there is the concept of a mesh or grid on which the computation is performed. To solve any problem by using FLUENT 12.1 code, a pre-processor code is used to create a computational mesh on which the equations can be solved.

In the present work, mesh tool GAMBIT was used and a two dimensional structured meshes (quadrilateral) were selected and the grid is close to the leading and trailing edges. The pressure and the suction sides of the blade should also be adequately clustered as shown in Fig. (4).

The (SST  $k - \omega$ ) turbulence model derived from the instantaneous Navier-Stokes equations was recommended by Ref. [16] to model the turbulence in the CFD code for the problem under investigation. A more comprehensive description of SST theory and its application to turbulence can be found in Ref. [17].

### **Theoretical calculation procedure**

The assumption suggested to the phase change model are, the homogeneous condensation, the droplet growth is based on average or mean radius, the droplet

surrounding is infinite vapor space, spherical droplet shape assumption and the heat capacity of the droplet is neglected compared with the latent heat released in condensation.

The mass generation rate due to condensation and evaporation  $\Gamma$  is given by the summation of mass increase due to formation of critical sized droplets (nucleation) and growth of these droplets [18] as follows:

$$\Gamma = \frac{4}{3}\pi\rho_l I r^{*3} + 4\pi\rho_l \eta \bar{r}^2 \frac{\partial \bar{r}}{\partial t} \quad \dots(3)$$

Where

$\bar{r}$  is the average radius of the droplet, (t) is the time, and ( $r^*$ ) is the Kelvin-Helmholtz critical droplet radius which given by:

$$r^* = \frac{2\sigma}{\rho_l R T_g \ln S} \quad \dots(4)$$

Where

S is the super saturation ratio defined as the ratio of vapor pressure to the equilibrium saturation pressure. The expansion process is usually very rapid. Therefore, when the state path crosses the saturation vapor line then the process will be non-equilibrium, and the supersaturating ratio  $S > 1$ . The condensation process involves two mechanisms, the mass transport from the vapor to the droplets and heat transfer from the last to the surrounding in the form of latent heat and can be done by introducing the energy balance.

The classical homogeneous nucleation theory describes the formulation of a liquid – phase in the form of droplets from a supersaturated phase in the absence of impurities or foreign particles [18]. The nucleation rate is repeated until a converged solution to steady state is achieved.

The entire solution strategy for solving wet steam flow can now be summarized by the following steps:

**1-Solving the Navier-Stokes equations for mixture flow, using the density-based algorithm.** The wet steam is a mixture of two phases; the primary phase is the gaseous– phase consisting of water vapor while the secondary phase is the liquid–phase consisting of condensed water droplets. For simplicity of the analysis, the following assumptions are made in this model, no slip velocity between the droplets and Vapor surrounding them, the interactions between droplets are neglected, the wetness mass fraction is small, less than 20 and the liquid phase consists of droplets whose radii are on order of 1 $\mu$ m or less.

From the preceding assumptions, it follows that the mixture density ( $\rho$ ) can be related to the vapor density ( $\rho_g$ ) by the following equation;

$$\rho = \frac{\rho_g}{(1-\beta)} \quad \dots(5)$$

Where

$\beta$  is the wetness mass fraction factor of the condensing liquid phase. The transport equation governs the mass fraction of the condensed liquid phase is

$$\frac{\partial \rho \beta}{\partial t} + \nabla \cdot (\rho V \beta) = \Gamma \quad \dots(6)$$

The conservation of the droplets density

$$\frac{\partial \rho \eta}{\partial t} + \nabla \cdot (\rho V \eta) = \rho I \quad \dots (7)$$

2- In each control volume in the computational domain, CFD Code computed the source terms for equations (6) and (7), nucleation rate and mass generation relations.

3- The transport equations for liquid mass fraction and number of droplets then sequentially solved by using the procedure of the pressure-based method for unstructured meshes.

4- Update all properties.

### Results and Discussions

Test conditions Details of the experimental conditions for all the cascade tests are given in table 2. The speed of sound in a two phase mixture is not explicit, and its values depends on the local conditions, while the pressure can be directly measured. For this reason in two phase flows it is preferable to work in terms of static pressure ratio ( $P_s/P_o$ ), therefore the isentropic Mach number can be based on this ratio.

**Table (2) Test conditions Details of the experimental conditions for all the cascade tests**

Test No.	$P_{o \text{ in}}$ (bar)	$T_o$ (K)	$P_b$ (bar)
R1	0.5	355.13	0.3
R2	0.5	355.13	0.21
R3	0.5	355.13	0.17
R4	0.42	355.13	0.26
R5	0.42	355.13	0.2
R6	0.42	355.13	0.16

In particular the rapid condensation zone is seen to occur at the same position in all the tests. This is partly due to the extremely high rate of expansion of the flow in the throat followed by a sudden change immediately downstream. In addition it can be shown that for steam flowing in a constant area duct in the Mach number range of approximately 0.9-1 any heat addition due to condensation will accelerate the flow and cause the supercooling to increase.

The variation of the ratio of static pressure to total pressure ( $P_s/P_o$ ) with fraction of surface distance is shown in Figures (5 to 10). In these figures, the upper curves represent the pressure profile near the pressure surfaces of the blades; the lower curves show this parameter near the suction surfaces and the middle curves show the pressure profile at the middle passage distance.

The comparison with experimental data for the static pressure ratio shows good correspondence on the pressure side and reasonable for both the suction side and the middle passage distance. The concerned figures, show an over expansion in the throat on the suction surface. The pressure decreases more mildly on the pressure side rather than suction side.

On the suction surface, from the  $x$  position of zero to 0.05, because of the curve of blade in this location, the pressure fall down rapidly. Along the suction side, a shock occurs that has been captured reasonably. Also in the above figures it can be seen that any decrease in outlet pressure ( $P_b$ ), will cause decrease in static pressure ratio i.e. more nucleation zone and liquid phase mass fraction to increase.

Figures (11-12) show the variation in liquid mass generation rate in the computational domain. Low back pressure cause high liquid mass generation rate for all ranges of inlet superheat conditions. As the rate of expansion increased a results of more departures from thermodynamic equilibrium and the superheated steam crosses the saturation line and becomes saturated steam. From these figures it can be seen that the maximum liquid mass generation rate have a low values of order of  $10^{-12}$  and  $10^{-15}$ , since the outlet flow either to be subsonic or sonic, Figures (11-a) and (12- a), because the steam is remains in superheated zone; therefore there is no departure from thermodynamic equilibrium or nearly so.

Figures (13-14) show that the computed droplets nucleation rate is increased as the back pressure decreased. The droplets nucleation rate occurred downstream away of the throat and move toward the throat as the back pressure is decreased. The position of the maximum values of the droplets nucleation rate is mostly occurred downstream the throat in the rapid condensation zone and continuing increasing in high rate with continous decrease in back pressure.

Figures (15-16) show that the computed droplets growth rate is increased as the back pressure decreased. The droplets growth rate occurred downstream away of the throat and move toward the throat as the back pressure is decreased. The position of the maximum values of the droplets growth rate is mostly occurred downstream the throat in the rapid condensation zone and continuing increasing in high rate with continuing decreasing the back pressure.

The condensation zone occurred downstream the throat area due to the reduction of the back pressure. As a matter of fact the dominant effect of phase change in high speed condensing flows is the local departures from thermodynamic equilibrium associate with the sudden release of heat from the droplets. The internal heat transfer associated with phase change is thermodynamically an irreversible process. It is particularly very extreme during the nucleation process that incurs an entropy increase associated with increase in stagnation temperature and hence a loss in work potential.

It is well known that the release of the latent heat by the homogenously nucleating steam flow can have a strong effect on the flow dynamics when the flow is transonic or supersonic with shock waves present. When the outlet flow is supersonic the heat release from the droplets causes a pressure rise in the zone of rapid condensation in the blade suction side

### **Concluding Remarks**

The paper has described an experimental study of the non-equilibrium flow of condensing steam in a stationary cascade of turbine blades operating transonically. A detailed comparison of the experimental data with condensing flow theory was also undertaken using a two-dimensional inviscid finite volume computer program. Excellent agreement was obtained throughout and, on the evidence presented, it can be stated that the theory and calculation procedure reproduce accurately all the main features of steady transonic condensing flow in stationary cascades, including the complex interactions occurring between the trailing edge shock wave system and the regions of nucleation and rapid droplet growth.

The most important influence of rapid condensation on the pressure distribution is experienced on the suction surface. But in the numerical results when the flow is regard subsonic flow the rapid condensation zone still occurs downstream the throat and not accompanied by a pressure rise, while in the experimental results for same case there is

no indication of this condensation. When the outlet is termed supersonic, the heat release causes a pressure rise in the zone of rapid condensation.

Finally, the results presented in this paper demonstrate that the two-dimensional non-equilibrium theory and calculation procedures that have been developed will predict quantitatively the complex steam flows of transonic turbine blading. A fully three-dimensional non-equilibrium analysis for a multi-stage steam turbine is still a long way in the future but the work presented in this paper represents a step in that direction.

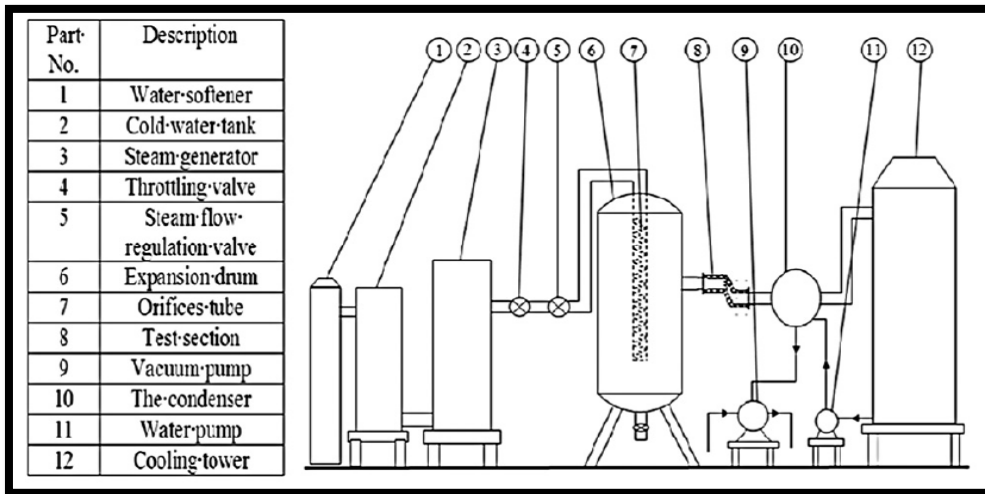


**Figure (1): Schematic diagram of the system**

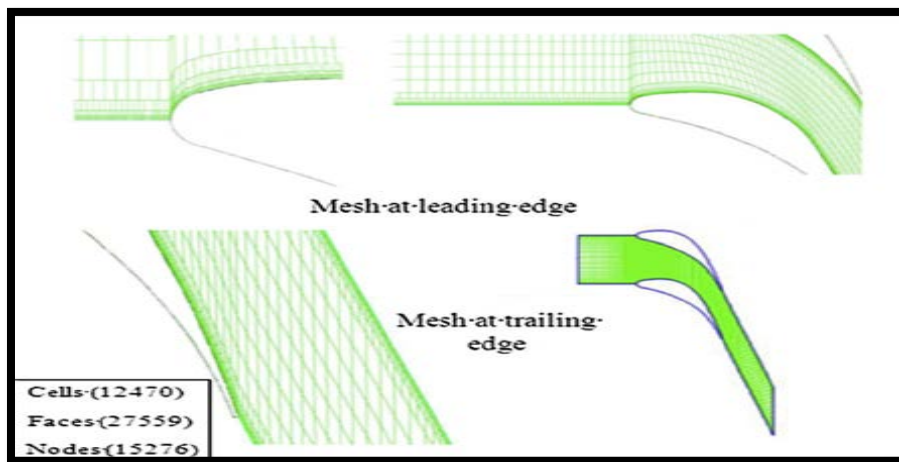


**Figure (2): cascade test section arrangement**

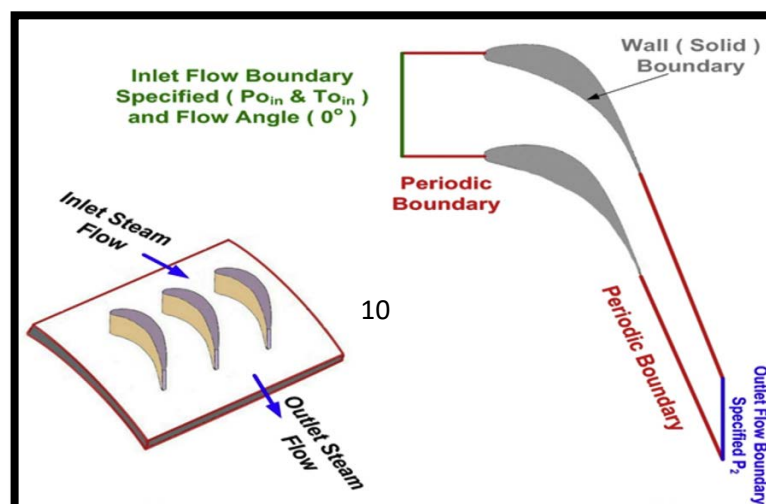


**Figure (3): Boundary conditions**

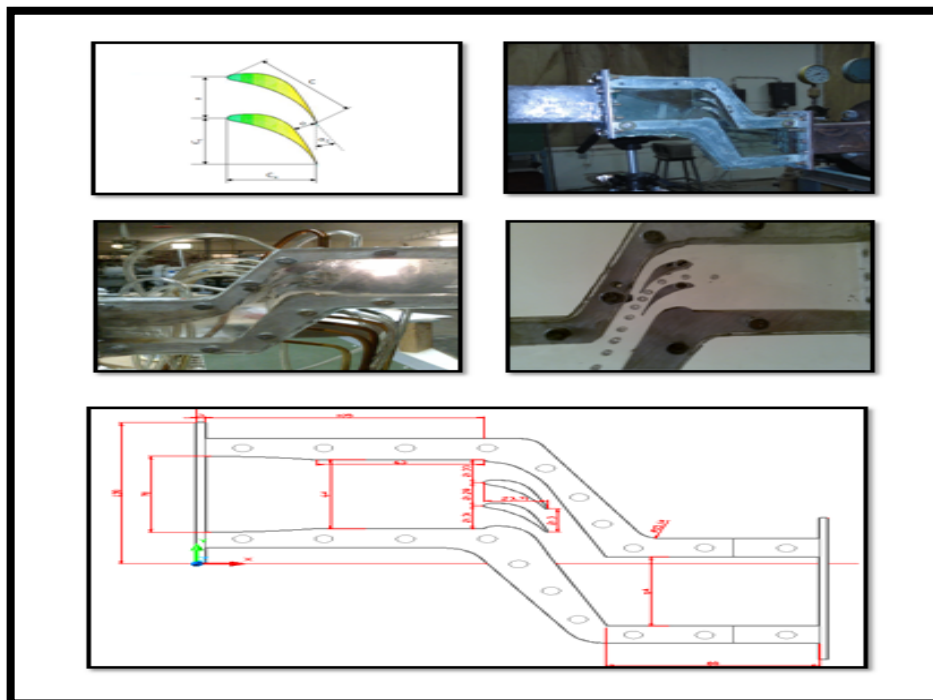


**Figure (4): Computational domain**

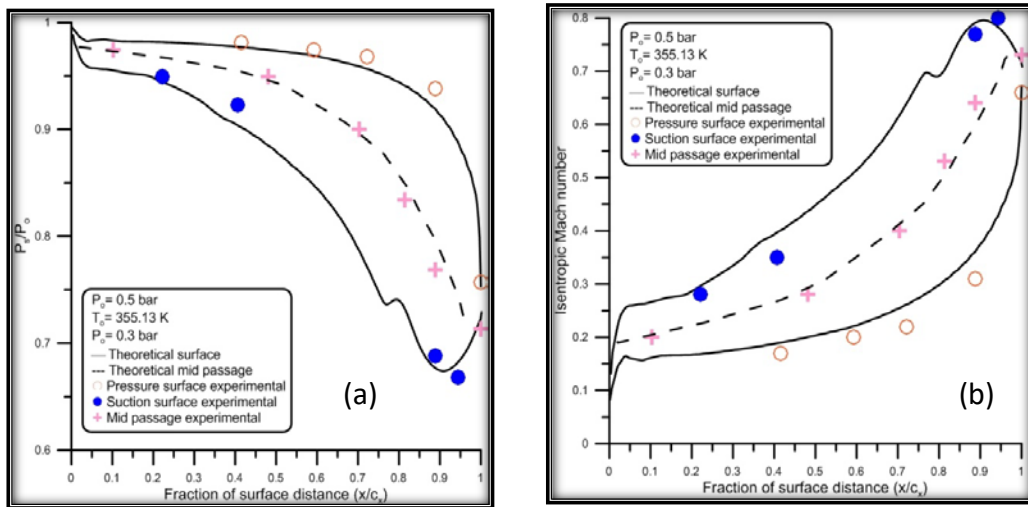


Figure (5) variation of (a) blade surface static pressure ratio, (b) Blade surface isentropic Mach number with fraction of surface distance.

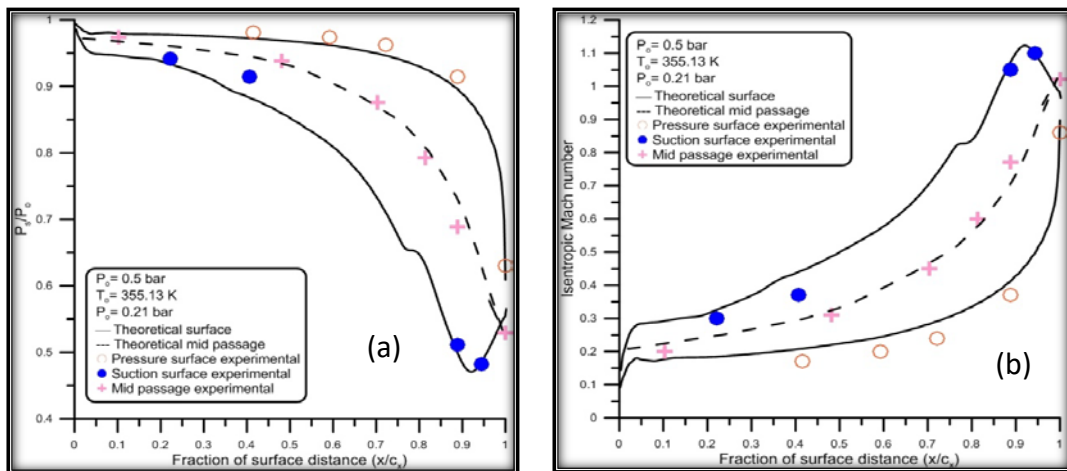


Figure (6) variation of (a) blade surface static pressure ratio, (b) Blade surface isentropic Mach number with fraction of surface distance.

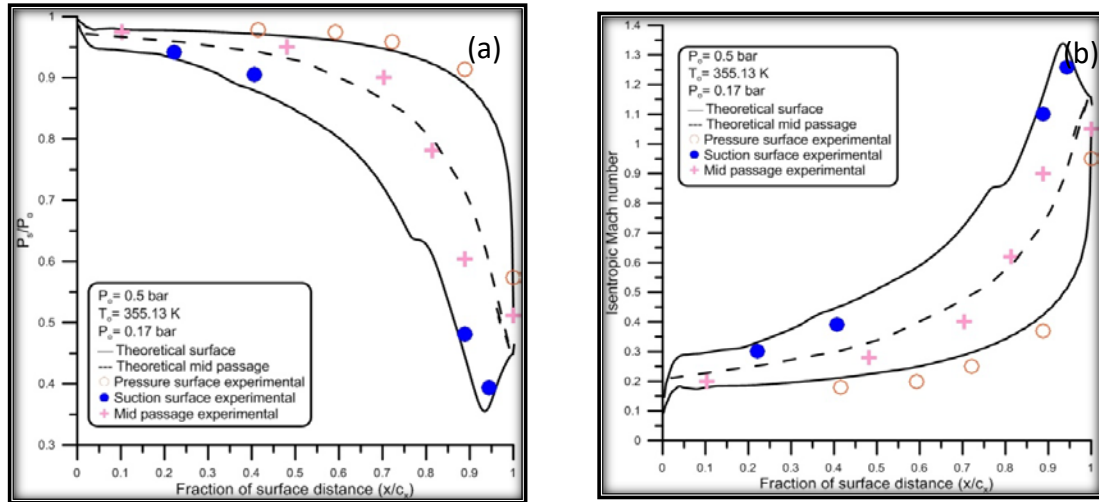


Figure (7) variation of (a) blade surface static pressure ratio, (b) Blade surface isentropic Mach number with fraction of surface distance.

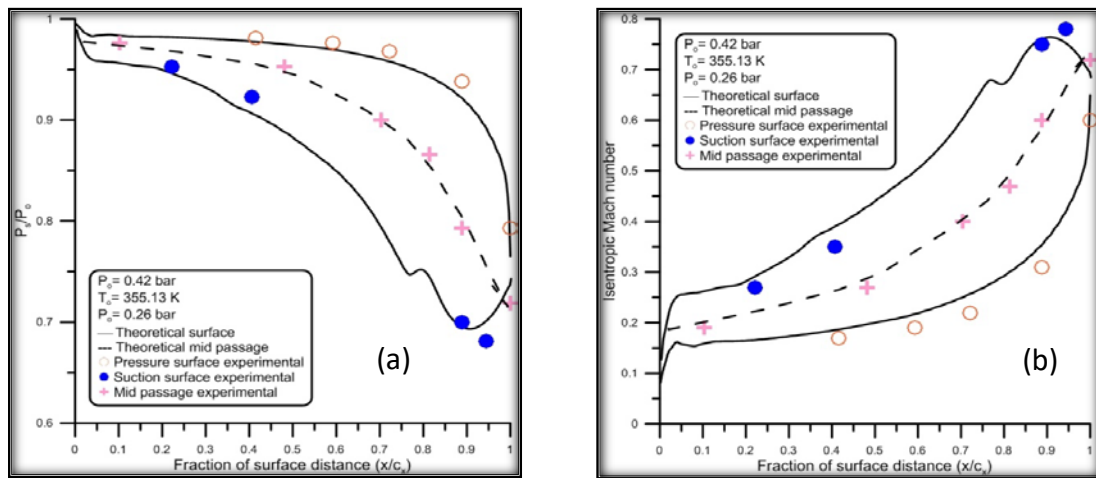


Figure (8) variation of (a) blade surface static pressure ratio, (b) Blade surface isentropic Mach number with fraction of surface distance.

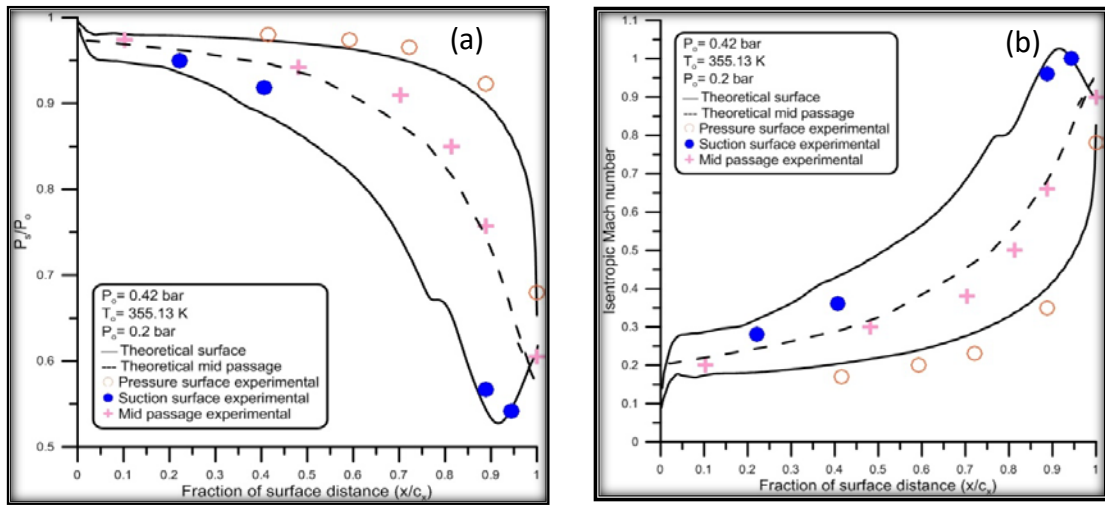


Figure (9) variation of (a) blade surface static pressure ratio, (b) Blade surface isentropic Mach number with fraction of surface distance.

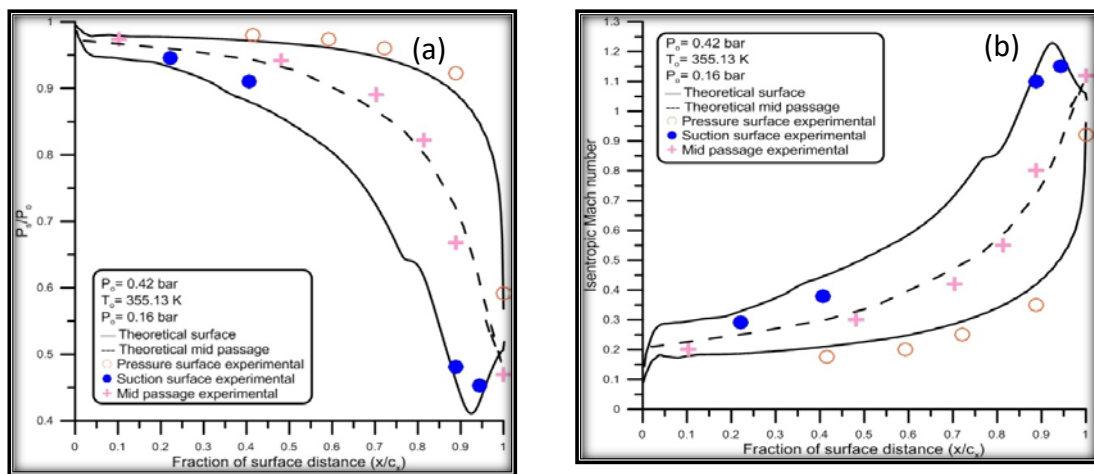


Figure (10) variation of (a) blade surface static pressure ratio, (b) Blade surface isentropic Mach number with fraction of surface distance.

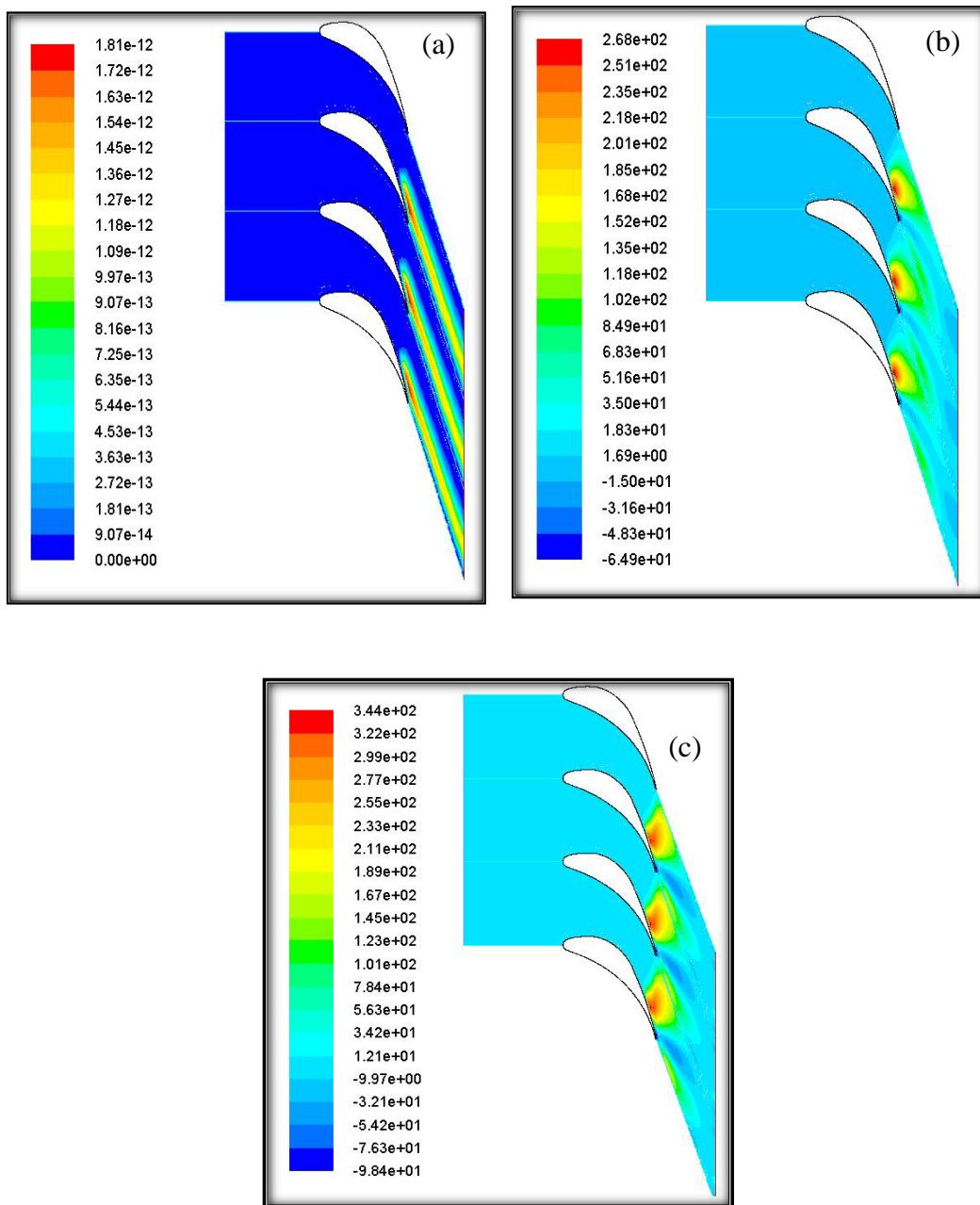


Figure (11) liquid mass generation rate contours ( $\text{kg/m}^3 \cdot \text{s}$ ) For tests (a) R1, (b) R2 and (c) R3.

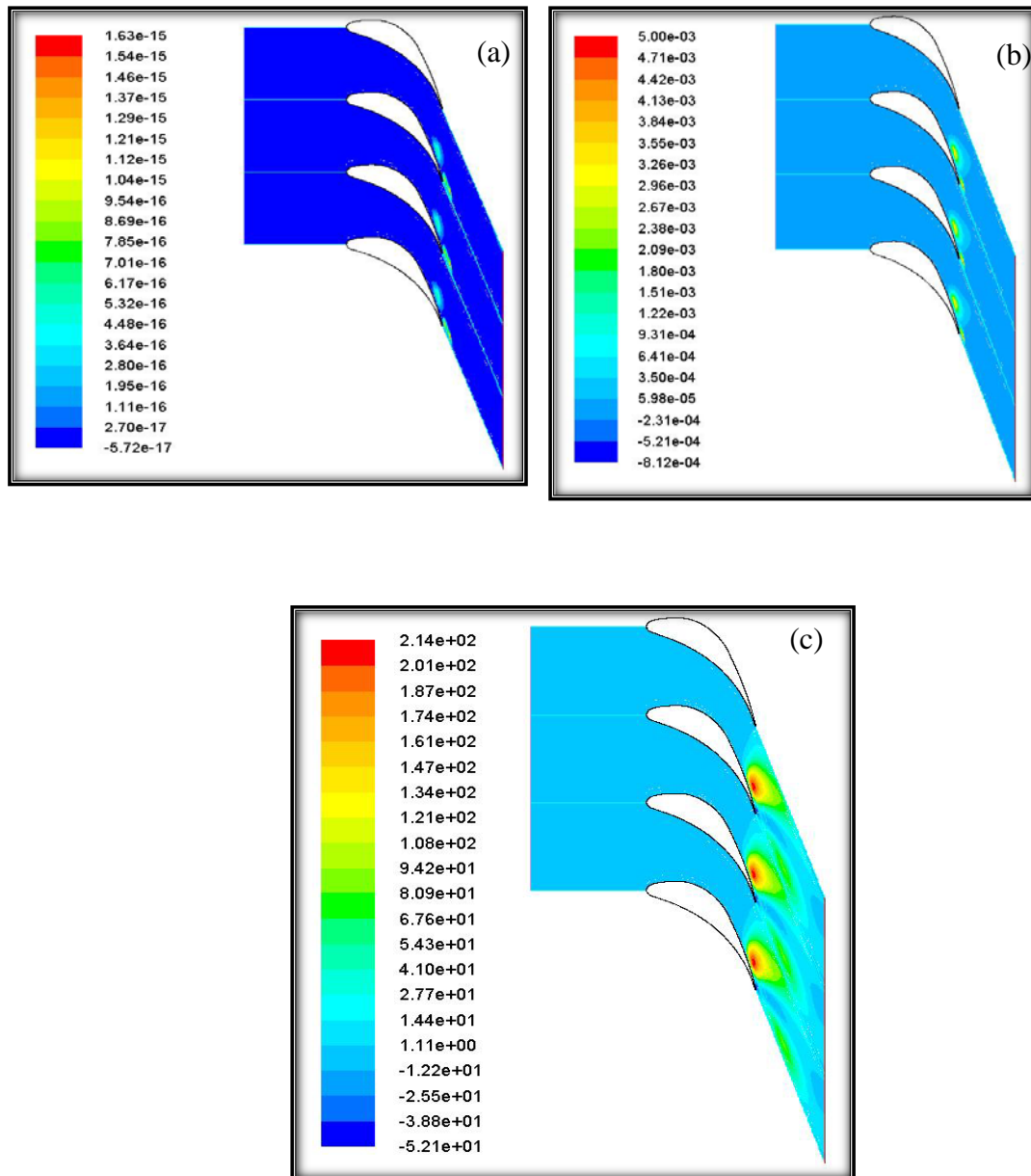
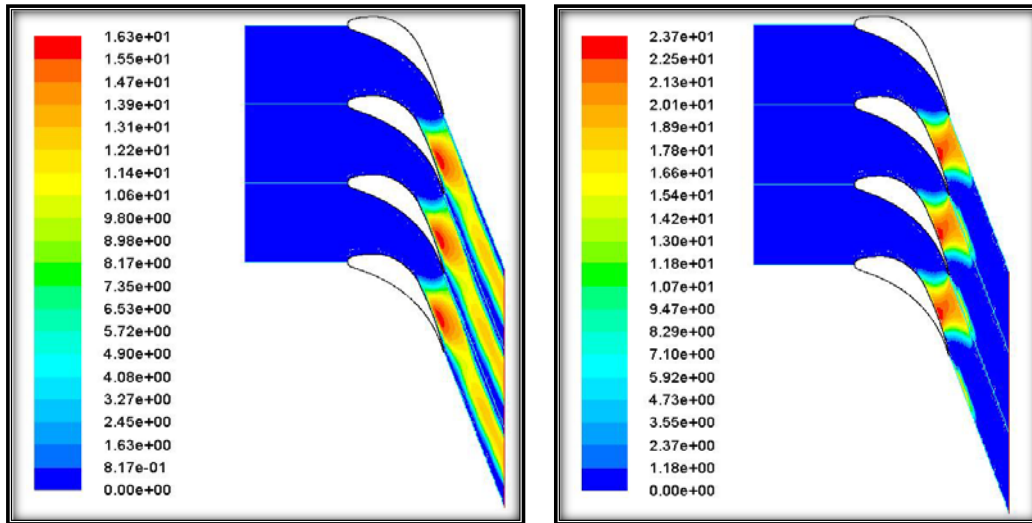
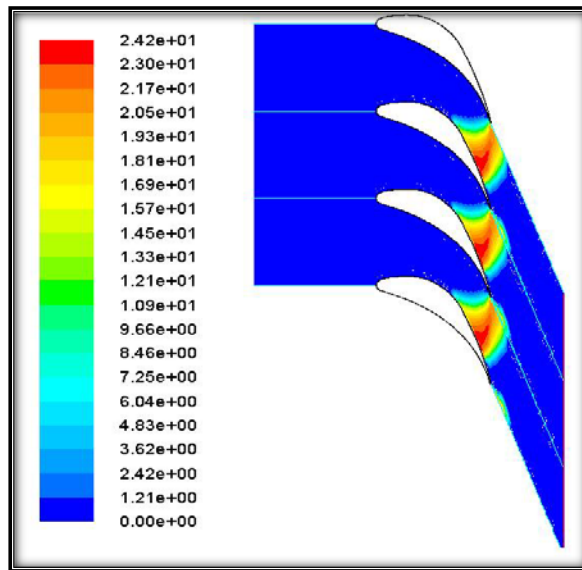


Figure (12) Liquid mass generation rate contours ( $\text{kg/m}^3 \cdot \text{s}$ ) For tests (a) R4, (b) R5 and (c) R6.



(a)

(b)



(c)

Figure (13)  $\log_{10}$  droplet nucleation rate contours for tests (a) R1, (b) R2 and (c) R3.

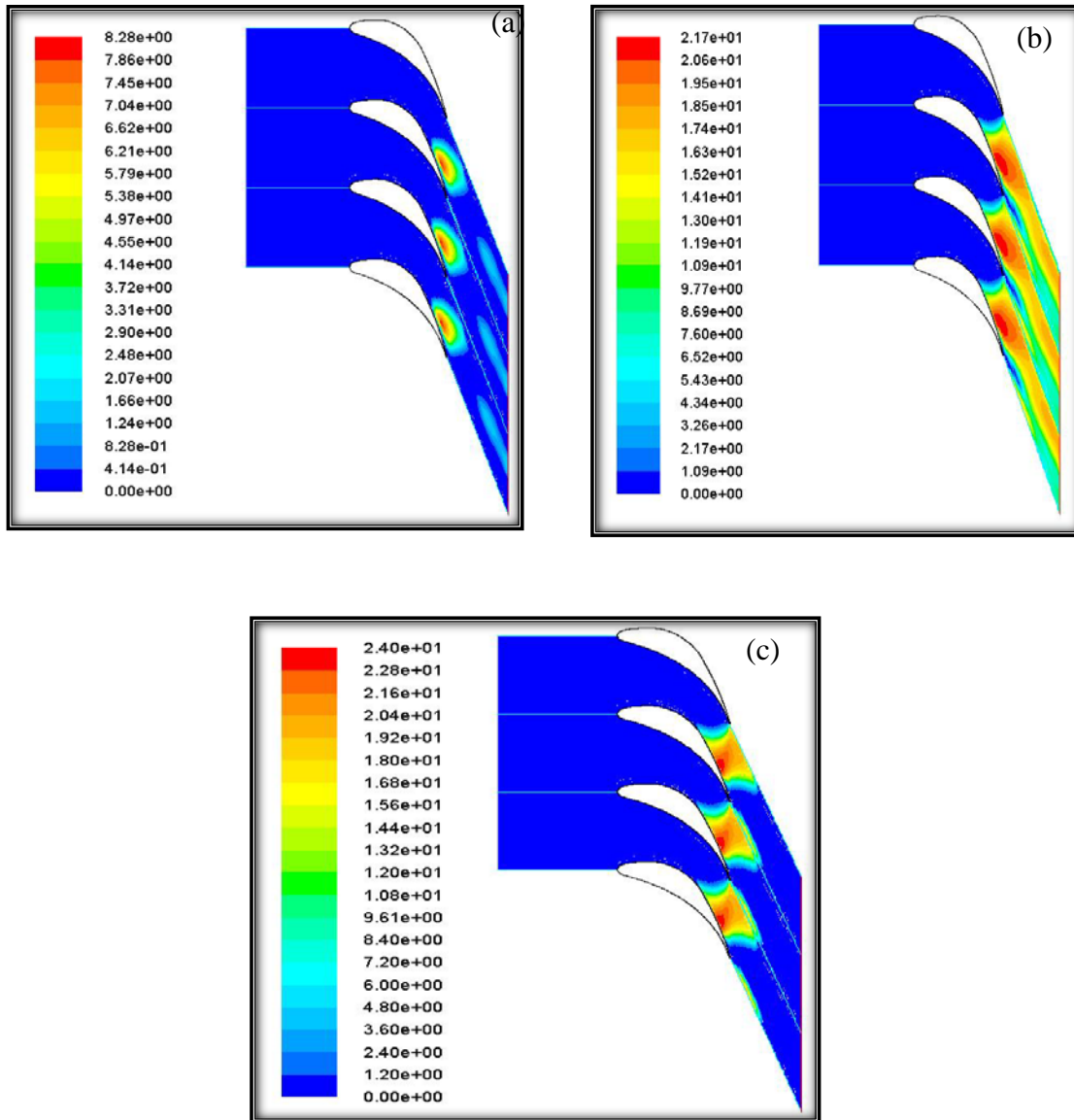


Figure (14)  $\log_{10}$  droplet nucleation rate contours for tests (a) R4, (b) R5 and (c) R6.

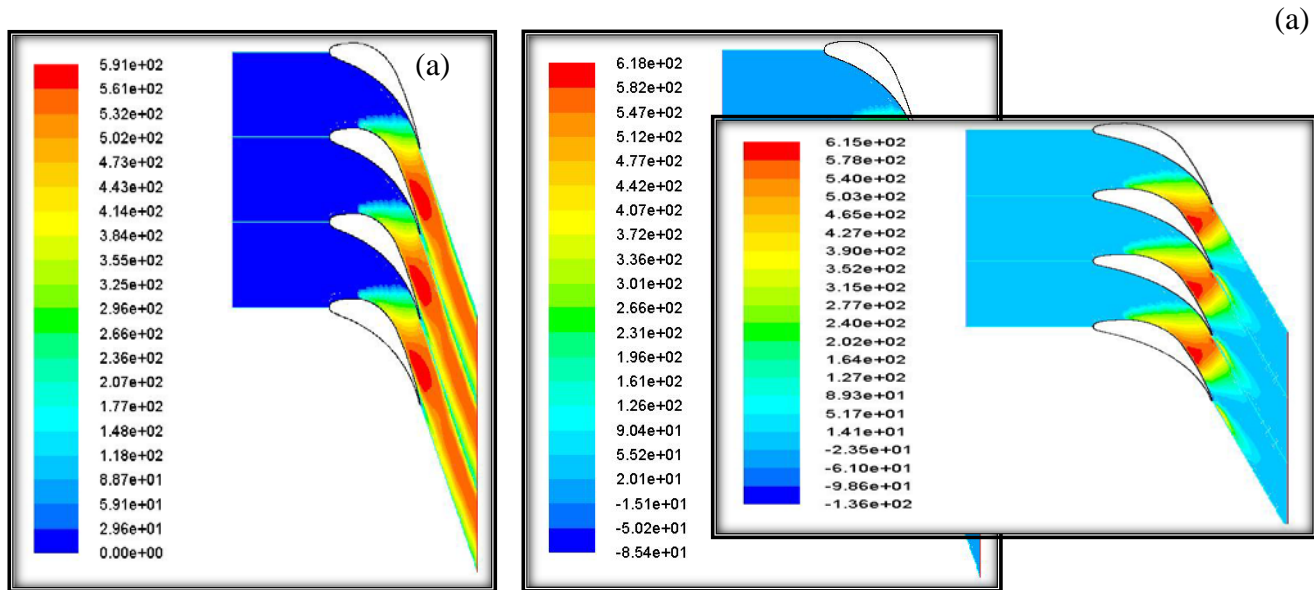


Figure (15) droplet growth rate contours (microns/s) for tests (a) R1, (b) R2 and (c) R3.

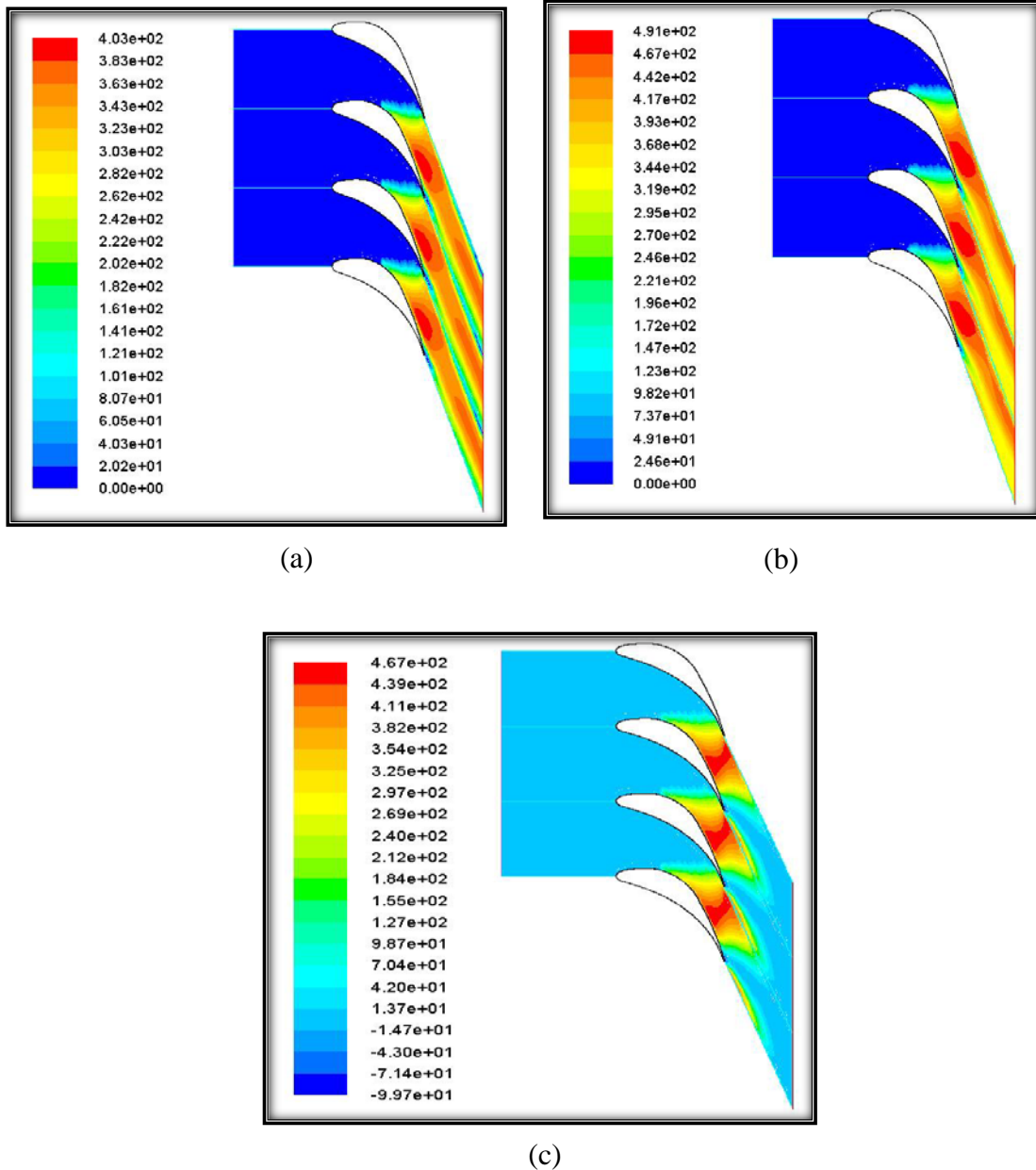


Figure (16) droplet growth rate contours (microns/s) for tests (a) R4, (b) R5 and (c) R6.

### References

- [1] Young, J. B. (The spontaneous condensation of steam in supersonic nozzles). PCH Phys. Chem. Hydrodynam. 3, 57-82.(1982).
- [2] Walters, P. T. (Optical measurement of water droplets in wet steam). Instn. Mech. Engrns Conf. (Warwick 1973) paper no. C32/73. In Wet Steam 4, 32-40.(1973)

- [3] Walters. P. T. (Wetness and efficiency measurements in LP turbines with an optical probe as an aid to improving performance). Joint ASME/IEEE Conf. on Power Generation (Milwaukee 1985), paper no. 85-JPGC-GT-9.(1985).
- [4] Walters, P. T. (Practical applications of inverting spectral turbidity data to provide aerosol size distributions). Appl. Optics 19, 2353-2365. ( 1980)
- [5] F. Bakhtar, M. Ebrahimi and R.A. Webb: (on the performance of a cascade of turbine rotor tip section blading in nucleating steam, part 1: surface pressure distributions), Proc. Instn. Mech. Engrs., Vol. 209, pp. 115-124. (1995).
- [6] A.J. White, J.B. Young and P.T. Walters:(Experimental validation of condensing flow theory for a stationary cascade of steam turbine blades), Phil. Trans. Roy. Soc. Series A, 354, pp.59-88, (1996).
- [7] A.H. Yousif, A.M. Al- Dabagh and R.CH. Al-Zuhairy: (Non-equilibrium spontaneous condensation in transonic steam flow), International Journal of Thermal Sciences. Vol. 68, pp.32-41, (2013).
- [8] M.Y. Zamri, H. Ibrahim, M.I. Azree, (Prediction and Improvement of Steam Turbine Performance Using Computational Fluid Dynamics), Department of Mechanical Engineering College of Engineering University Tenaga Nasional (UNITEN).(2000).
- [9] S. Dykas, (Numerical calculation of the steam condensing flow), TASK Quarterly 5 (4) 519-535. (2001).
- [10] Liang Li, Guojun Li, Z. Feng, (Numerical simulation of spontaneously condensing flows in a plane turbine cascade), TASK Quarterly 6 (1) (2002) 209-216.
- [11] A.G. Gerber, M.J. Kermani, (A pressure based Eulerian-Eulerian multi-phase model for non-equilibrium condensation in transonic steam flow), International Journal of Heat and Mass Transfer 47 (2004) 2217-2231.
- [12] K.C. Ng, M.Z. Yusoff, T.F. Yusaf, Simulation of two-dimensional high speed turbulent compressible flow in a diffuser and a nozzle blade cascade, American Journal of Applied Sciences 2 (9) 1325-1330. (2005)
- [13] L. Zori, F. Kececy, (Wet Steam Flow Modeling in a General CFD Flow Solver), 35th AIAA (American Institute of Aeronautics and Astronautics) Fluid Dynamics Conference, pp. 1-15. (2005).
- [14] S. Senoo, A.J. White, (Numerical Simulations of Unsteady Wet Steam Flows with Non-equilibrium Condensation in the Nozzle and the Steam Turbine), ASME Joint U.S. European Fluid Engineering, Summer Meeting, July 17-20. (2006).
- [15] A.G. Gerber, (In homogeneous multi fluid model for prediction of non equilibrium phase transition and droplet dynamics), Journal of Fluids Engineering 130.(March 2008).
- [16] A.H. Yousif, H. Tarteb, (Validation of numerical computations and turbulence models combinations for gas turbine cascade blade flow), Engineering and Technology Journal 29 (14). (2011).
- [17] F. R. Menter. (Two-Equation Eddy-Viscosity Turbulence Models for Engineering Applications). AIAA Journal, 32(8):1598-1605, August (1994).
- [18] I.J. Ford, Nucleation theorems, the statistical mechanics of molecular clusters and a revision of classical nucleation theory, Physical Review E 56, 5615-5629. (1997).